# High order finite element simulations for fluid dynamics validated by experimental data from the fda benchmark nozzle model

Vincent Chabannes, Christophe Prud'Homme, Marcela Szopos, Ranine Tarabay

# HIGH ORDER FINITE ELEMENT SIMULATIONS FOR FLUID DYNAMICS VALIDATED BY EXPERIMENTAL DATA FROM THE FDA BENCHMARK NOZZLE MODEL

**V. Chabannes, C. Prud'homme, M. Szopos, and R. Tarabay**
Université de Strasbourg, CNRS, IRMA UMR 7501, F-67000 Strasbourg, France,
{chabannes,prudhomme,szopos,tarabay}@math.unistra.fr

**SUMMARY**

The objective of the present work is to construct a sound mathematical, numerical and computational framework relevant to blood flow simulations and to assess it through a careful validation against experimental data. We perform simulations of a benchmark proposed by the FDA for fluid flow in an idealized medical device, under different flow regimes. The results are evaluated using metrics proposed in the literature and the findings are in very good agreement with the validation experiment.

**Key words:** *CFD, validation, medical device, open source finite element software*

## 1 INTRODUCTION

A challenging benchmark was proposed by the US Food and Drug Administration (FDA) in [1] in order to assess the stability, accuracy and robustness of computational methods in different physiological regimes. The findings of 28 blinded investigations were reported in [2] and as critically analyzed in [3], practically all CFD solvers failed to predict results that agreed in a satisfactory manner with the experimental data. Several subsequent papers tackled this question, by employing different numerical approaches: for instance a finite-element based direct numerical simulation method in [4] or a large-eddy simulation method in [5].

We aim at contributing to the effort of improving the reliability and reproducibility of computational studies by performing a thorough validation of the fluid solver developed in the open source finite element library Feel++ [6]. In the current investigation, we present results corresponding to three Reynolds numbers $500, 2000$ and $3500$ obtained by using a direct numerical simulation method of the Navier-Stokes equations. In particular we implement and compare low order as well as high order approximations including for the geometry and we discuss some issues not previously reported in the literature.

| $\mathcal{R}e_i$ | $\mathcal{R}e_t$ | FLOW RATE |
|---|---|---|
| 167 | 500 | $5.21 \cdot 10^{-6}$ |
| 667 | 2,000 | $2.08 \cdot 10^{-5}$ |
| 1,167 | 3,500 | $3.64 \cdot 10^{-5}$ |

Figure 1: Computational domain (top) and flow regime specifications (bottom); $\mathcal{R}e_i$ and $\mathcal{R}e_t$: Reynolds number in the inlet section and throat section, respectively.

## 2 METHODOLOGY

**Benchmark description.** The FDA benchmark nozzle model provides a comprehensive dataset of experimental measures using a well-defined geometry corresponding to an idealized medical device

(see Figure 1 for a schematic sketch of the domain and [1, Sec. 2.1] for the precise dimensions of each part). Five sets of data spanning laminar, transitional and turbulent regimes are made available; we focus in the current work on the flow regime specifications described in Figure 1.

The comparison with experimental data is made in terms of (i) wall pressure difference (normalized to the mean throat velocity) versus axial distance; and (ii) axial component of the velocity (normalized to the mean inlet velocity) along the centerline:

$$\Delta p^{norm} = \frac{p_z - p_{z=0}}{\frac{1}{2}\rho_f \overline{u}_t^2} \text{ and } \quad u_z^{norm} = \frac{u_z}{\overline{u}_i}, \text{ where } \quad \overline{u}_t^2 = \frac{4Q}{\pi D_t^2}, \; \overline{u}_i = \frac{4Q}{\pi D_i^2}, \tag{1}$$

and $Q$ is the volumetric flow rate retrieved from $\mathcal{R}e_t$ (see Figure 1, right panel). Furthermore, we present results on two validation metrics reported in [2], also assessed in [4]: a conservation of mass error metric $E_Q$ (on a percentage basis) and a general validation metric $E_z$ comparing average experimental velocity data with computed axial velocities.

**Fluid equations and numerical approach.** We now turn to the mathematical and the numerical setting. We consider the homogeneous, incompressible, unsteady Navier-Stokes equations, which read in conservative form: find $(\mathbf{u}, p)$ such that $\rho\left(\frac{\partial \mathbf{u}}{\partial t} + (\mathbf{u}\cdot\nabla)\mathbf{u}\right) - \mu\Delta\mathbf{u} + \nabla p = \mathbf{0}, \quad \text{div}(\mathbf{u}) = 0,$ in $\Omega \times I$. The set $\Omega \subset \mathbb{R}^3$ represents the spatial domain described in Figure 1. $I = (0, T)$ is the time interval, $\mathbf{u}$ and $p$ are the velocity and pressure of the fluid and $\rho$ and $\mu$ are the density and the dynamic viscosity of the fluid, respectively. We supplement the equations with initial and boundary conditions. At $t = 0s$, the fluid is considered to be at rest, $\mathbf{u}(\mathbf{x}, t) = \mathbf{0}$. A Poiseuille velocity profile is imposed on $\Gamma_{\text{inlet}}$, homogeneous Dirichlet condition on $\Gamma_{\text{wall}}$ and a free outflow on $\Gamma_{\text{outlet}}$.

We refer to [8, Sec. 2] regarding the variational formulation, the finite element discretization including low to high order geometry as well as the time discretization. We choose the generalized Taylor-Hood finite element for the velocity-pressure discretization; the notation $P_{N+1}P_N G_{k_{\text{geo}}}$ is used to specify exactly the discretization spaces for the velocity, pressure and geometry, respectively.

The benchmark hereafter is developed in the framework of the Finite Element Embedded Library in C++, Feel++[6], that allows to use a very wide range of Galerkin methods and advanced numerical techniques such as domain decomposition. The ingredients include a very expressive embedded language, seamless interpolation, mesh adaption and seamless parallelization. Regarding the computational domain, we used GMSH. The construction used the following steps: *(i)* start with a 2D geometry embedding the benchmark metric locations and customizing characteristic mesh size depending on the region and *(ii)* extrude by rotation to obtain the device geometry. Finally we use the PETSc interface developed in Feel++ and in particular the FieldSplit preconditioning framework to implement block preconditioning strategies such as PCD [7]. Note that PCD requires specific tuning with respect to boundary conditions.

## 3 RESULTS AND CONCLUSIONS

We perform simulations for three Reynolds numbers evaluated in the throat $\mathcal{R}e_t = 500, 2000, 3500$, with several mesh refinements and polynomial order approximations. The fluid's prescribed density is $\rho = 1056\frac{kg}{m^3}$ and viscosity $\mu = 0.0035 Pa.s$. The mesh characteristics are described in Table 1. At $\mathcal{R}e_t = 500$, the simulation is carried out until $t = 3s$, time reasonably close to the steady state, and we choose the time step equal to $\Delta t = 10^{-3}$. At $\mathcal{R}e_t = 2000$ (resp $\mathcal{R}e_t = 3500$), the numerical experiments were carried out until $t =$

| | $h_{min}$ | $h_{max}$ | $h_{average}$ | $N_{\text{elt}}$ |
|---|---|---|---|---|
| M0 | $1.9 \cdot 10^{-4}$ | $2.9 \cdot 10^{-3}$ | $1.3 \cdot 10^{-3}$ | 412 575 |
| M1 | $1.6 \cdot 10^{-4}$ | $1.8 \cdot 10^{-3}$ | $7.6 \cdot 10^{-4}$ | 830 000 |
| M2 | $1.4 \cdot 10^{-4}$ | $1.96 \cdot 10^{-3}$ | $6 \cdot 10^{-4}$ | 3 400 000 |
| M3 | $8.5 \cdot 10^{-5}$ | $1.7 \cdot 10^{-3}$ | $3.5 \cdot 10^{-4}$ | 7 000 000 |
| M4 | $6.3 \cdot 10^{-5}$ | $2.0 \cdot 10^{-3}$ | $5.8 \cdot 10^{-4}$ | 2 879 365 |
| M5 | $1.4 \cdot 10^{-4}$ | $2.6 \cdot 10^{-3}$ | $4.1 \cdot 10^{-4}$ | 3 200 000 |

Table 1: Characteristic lengths of the different meshes: $h_{min}, h_{max}, h_{average}$ are respectively the minimum, maximum and average edge length in the meshes and $N_{\text{elt}}$ is the number of tetrahedra.

$0.45s$ (resp $t = 0.4s$), time when the turbulent regime was fully developed and we set $\Delta t = 10^{-4}$.

Figure 2 shows the results in the three flow regimes for the normalized axial velocity and the normalized pressure difference along the $z$ axis, respectively. In each case, we can see satisfactory agreement with the experimental data. However, for $\mathcal{R}e_t = 2000$, we observe that the numerical jet breakdown point is captured further downstream than the experimentally observed breakdown point. As recently highlighted in [5], the prediction of the axial location of the jet breakdown is extremely sensitive to numerical parameters, therefore a possible explanation of this mismatch may be the accuracy of the numerical integration. Finally, we illustrate in Figure 3 the computation of metrics $E_z$ and $E_Q$ for several mesh refinements at $\mathcal{R}e_t = 500$. The metric $E_z$ takes small values in each numerical experiment, identifying a good agreement betweeen computed and experimental data, and displays only small variations with respect to mesh refinement. On the other hand, the metric $E_Q$ is more sensitive to this factor: error doesn't exceed the $\sim 2\%$ except for the coarse mesh $M0$ where, in two locations, the error increases up to $\sim 10\%$. Furthermore, we note that the $P_3P_2G_1$ approximation doesn't improve the results for the coarse mesh, but that a satisfactory error below $2\%$ is retrieved when using a $P_2P_1G_2$ approximation. Additional tests to complement the study of the impact of high order approximation are ongoing.

**Conclusions and perspectives** We validated our computation fluid dynamic framework against this FDA benchmark for three different regimes and different discretization and solution strategies. Perspectives include a full report on our findings including in terms of iteration and timing performances as well extending our results to the turbulent range.

**Acknowledgments** The authors wish to thank Mourad Ismail for the fruitful discussions we had. Moreover we would like to acknowledge the support of *(i)* Center of Modeling and Simulation of Strasbourg (Cemosis), *(ii)* the ANR MONU-Vivabrain *(iii)* the LabEx IRMIA and *(iv)* PRACE for awarding us access to resource Curie based in France at CCRT as well as GENCI for awarding us access to resource Occigen based in France at Cines

## REFERENCES

[1] P. Hariharan, M. Giarra,V. Reddy, S.W. Day, K.B. Manning, S. Deutsch, S.F.C. Stewart, M. Y. Myers, M.R. Berman, G.W. Burgreen, E.G Paterson, and R.A. Malinauskas. Multilaboratory particle image velocimetry analysis of the FDA benchmark nozzle model to support validation of computational fluid dynamics simulations. *Journal of Biomechanical Engineering*, 133(4):1–14, 2011.

[2] S.F.C. Stewart, P. Hariharan, E.G. Paterson, G.W. Burgreen, V. Reddy, S.W. Day, K.B. Manning, S. Deutsch, M.R. Berman, M. Y. Myers and R.A. Malinauskas. Results of FDAs first interlaboratory computational study of a nozzle with a sudden contraction and conical diffuser. *Cardiovascular Engineering and Technology*, 4(4):374–391, 2013.

[3] F. Sotiropoulos. Computational fluid dynamics for medical device design and evaluation: are we there yet?. *Cardiovascular Engineering and Technology*, 3(2):137–138, 2012.

[4] T. Passerini, A. Quaini, U. Villa, A. Veneziani and S. Canic. Validation of an open source framework for the simulation of blood flow in rigid and deformable vessels. *International journal for numerical methods in biomedical engineering*, 29(11):1192–1213, 2013.

[5] V. Zmijanovic, S. Mendez, V. Moureau and F. Nicoud. About the numerical robustness of biomedical benchmark cases: Interlaboratory FDA's idealized medical device. *International journal for numerical methods in biomedical engineering*, 33(1), 2017.

[6] C. Prud'homme, V. Chabannes, V. Doyeux, M. Ismail, A. Samake and G. Pena. Feel++: A Computational Framework for Galerkin Methods and Advanced Numerical Methods. *ESAIM: Proceedings, EDP Sciences*, 38:429–455, 2012.

[7] H.C. Elman, D.J. Silvester and A.J. Wathen. Finite elements and fast iterative solvers: with applications in incompressible fluid dynamics. *Oxford University Press (UK)*, 2014.

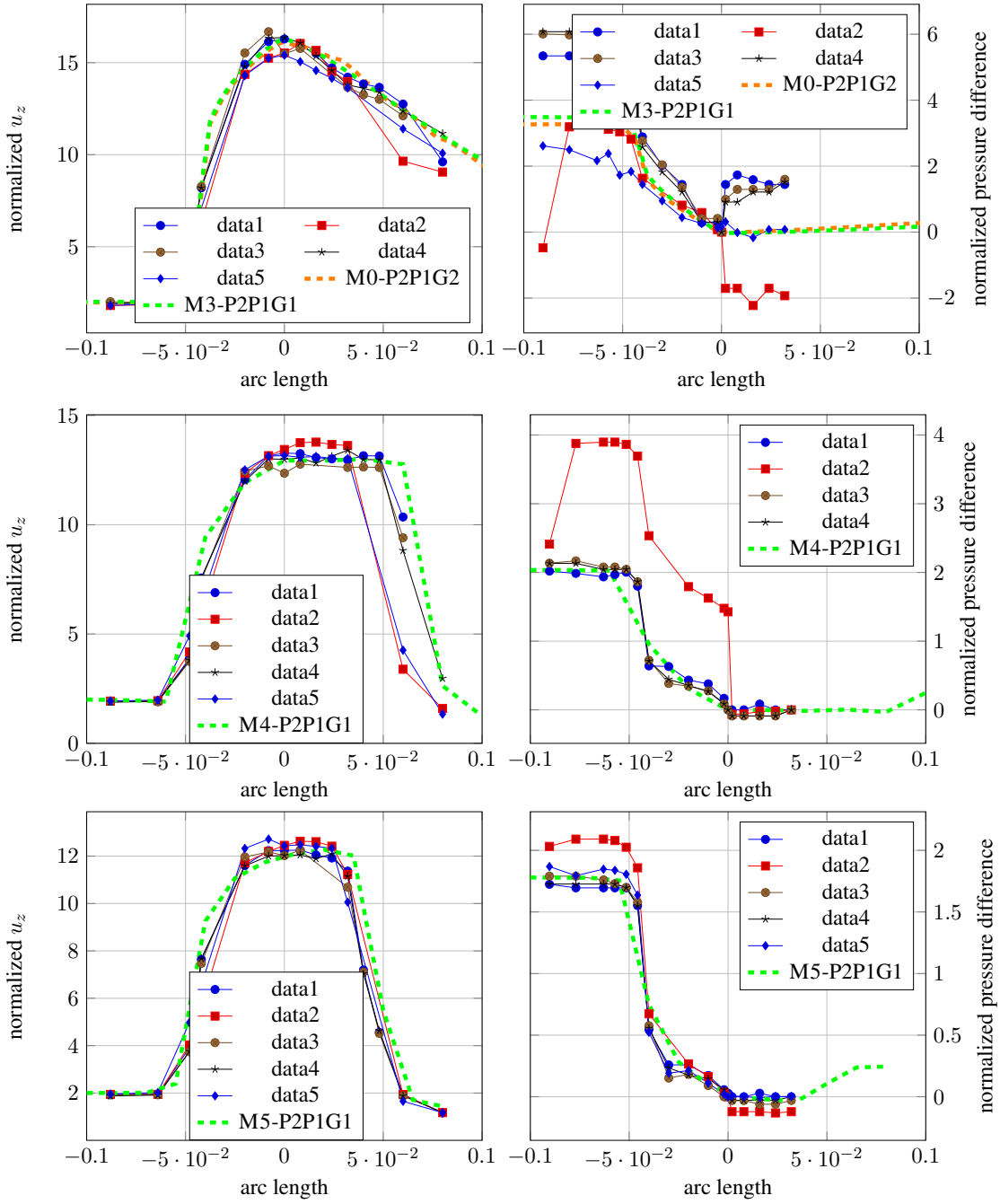


Figure 2: Comparison between experimental data and numerical results for the normalized axial velocity along z (left) and the normalized pressure difference along z (right), for $\mathcal{R}e_t = 500$ (top) $\mathcal{R}e_t = 2000$ (middle) and $\mathcal{R}e_t = 3500$ (bottom).

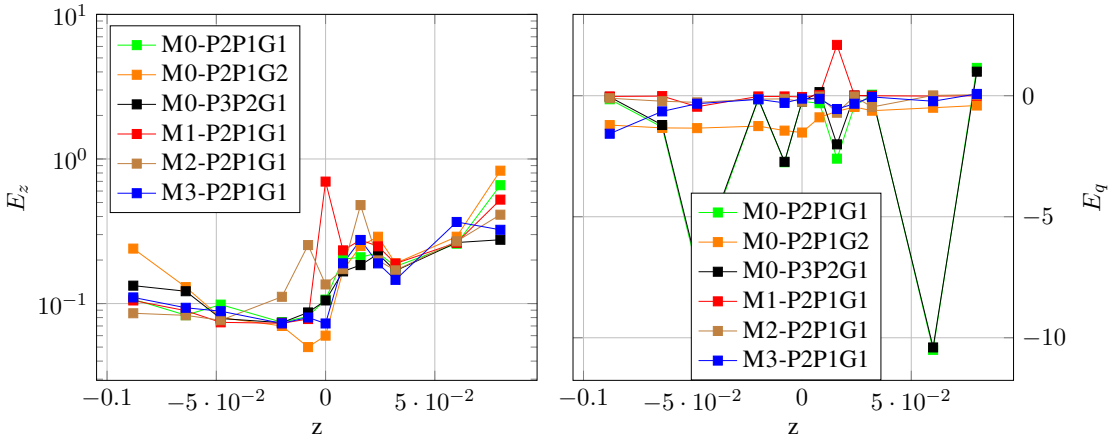


Figure 3: Validation metrics $E_z$ (left) and $E_Q$ (right) for $\mathcal{R}e_t = 500$.

[8] C. Caldini Queiros, V. Chabannes, M. Ismail, G. Pena, C. Prud'Homme, M. Szopos and R. Tarabay. Towards large-scale three-dimensional blood flow simulations in realistic geometries. *ESAIM: Proceedings, EDP Sciences*, 43:195–212, 2013.